mol) of 5-nitro-1-hydroxymethylnaphthalene in 20 mL of dry chloroform was added 0.06 mL (0.001 mol) of $\mathrm{SOCl_2}$ over a 30-min period with vigorous stirring. After stirring for an additional hour, the chloroform was removed by distillation. The residue, upon distillation under reduced pressure, gave the expected 5-nitro-1-chloromethylnaphthalene (mp 97 °C). The other halides were similarly prepared: 8-nitro-1-chloromethylnaphthalene,[28] 5-nitro-1-bromomethylnaphthalene (mp 98 °C), 8-nitro-1-bromomethylnaphthalene (mp 98 °C).

Registry No. p-$\mathrm{NO_2C_6H_4CH_2Cl}$, 100-14-1; p-$\mathrm{NO_2C_6H_4CH(CH_3)Cl}$, 19935-75-2; p-$\mathrm{NO_2C_6H_4CH_2Br}$, 100-11-8; p-$\mathrm{NO_2C_6H_4CH(CH_3)Br}$, 19935-81-0; p-$\mathrm{NO_2C_6H_4CHCl_2}$, 619-78-3; p-$\mathrm{NO_2C_6H_4CH_2OTs}$, 4450-68-4; p-$\mathrm{NO_2C_6H_4CH(CH_3)OTs}$, 82925-36-8; p-$\mathrm{NO_2C_6H_4CH_2CH_2Br}$, 5339-26-4; p-$\mathrm{NO_2C_6H_4CH_2CH(Ph)Br}$, 83966-28-3; p-$\mathrm{NO_2C_6H_4CH{=}CHCH_2Br}$, 75059-04-0; p-$\mathrm{NO_2C_6H_4CH{=}CHBr}$, 13161-29-0; m-$\mathrm{NO_2C_6H_4CH_2Cl}$, 619-23-8; m-$\mathrm{NO_2C_6H_4CH_2Br}$, 3958-57-4; $\mathrm{(CH_3)_2\dot{C}OH}$, 5131-95-3; p-$\mathrm{NO_2C_6H_4CH_2Cl}$ radical anion, 34509-98-3; p-$\mathrm{NO_2C_6H_4CH(CH_3)Cl}$ radical anion, 83966-31-8; p-$\mathrm{NO_2C_6H_4CH_2Br}$ radical anion, 34512-14-6; p-$\mathrm{NO_2C_6H_4CH(CH_3)Br}$ radical anion, 84024-96-4; p-$\mathrm{NO_2C_6H_4CHCl_2}$ radical anion, 83966-32-9; p-$\mathrm{NO_2C_6H_4CH_2OTs}$ radical anion, 83966-33-0; p-$\mathrm{NO_2C_6H_4CH(CH_3)OTs}$ radical anion, 83966-34-1; p-$\mathrm{NO_2C_6H_4CH_2CH_2Br}$ radical anion, 77145-96-1; p-$\mathrm{NO_2C_6H_4CH_2CH(Ph)Br}$ radical anion, 83966-35-2; p-$\mathrm{NO_2C_6H_4CH{=}CHCH_2Br}$ radical anion, 84024-97-5; p-$\mathrm{NO_2C_6H_4CH{=}CHBr}$ radical anion, 84024-98-6; m-$\mathrm{NO_2C_6H_4CH_2Cl}$ radical anion, 74261-77-1; m-$\mathrm{NO_2C_6H_4CH_2Br}$ radical anion, 74261-79-3; p-$\mathrm{NO_2C_6H_4CH_2\cdot}$, 19019-93-3; p-$\mathrm{NO_2C_6H_4CH(CH_3)\cdot}$, 83966-40-9; p-$\mathrm{NO_2C_6H_4CHCl\cdot}$, 83966-41-0; p-$\mathrm{NO_2C_6H_4CH_2\dot{C}HPh}$, 83966-42-1; p-$\mathrm{NO_2C_6H_4CH{=}CHCH_2\cdot}$, 83966-43-2; 1-(chloromethyl)-5-nitronaphthalene, 6625-54-3; 1-(chloromethyl)-8-nitronaphthalene, 19190-51-3; 1-(bromomethyl)-5-nitronaphthalene, 83966-29-4; 1-(bromomethyl)-8-nitronaphthalene, 83966-30-7; 1-(chloromethyl)-5-nitronaphthalene radical anion, 83966-36-3; 1-(chloromethyl)-8-nitronaphthalene radical anion, 83966-37-4; 1-(bromomethyl)-5-nitronaphthalene radical anion, 83966-38-5; 1-(bromomethyl)-8-nitronaphthalene radical anion, 83966-39-6; 8-nitronaphthanen-1-ylmethyl radical, 83966-44-3.

---

(28) Kleinfelter, D. C.; Chen, P. H. *J. Org. Chem.* **1969**, *34*, 1741.

Heterojunction Silicon/Indium Tin Oxide Photoelectrodes: Development of Stable Systems in Aqueous Electrolytes and Their Applicability to Solar Energy Conversion and Storage

G. Hodes,[†] L. Thompson, J. DuBow,[‡] and K. Rajeshwar*

Contribution from the Department of Electrical Engineering, Colorado State University, Fort Collins, Colorado 80525. *Received April 5, 1982*

Abstract: An approach to circumvent the problem of poor photoelectrochemical (PEC) stability of Si in aqueous electrolytes is the use of heterojunction photoelectrodes comprising the $\mathrm{Si/SiO}_x$/indium tin oxide (ITO) structure. As in a Schottky barrier electrode system, the maximum photovoltage attainable with these electrodes is limited by the barrier height at the Si/ITO heterojunction. Both n- and p-Si substrates have been studied. In regenerative PEC systems designed for the conversion of solar energy to electricity, the efficacy of charge transfer at the ITO/electrolyte interface is shown to be a crucial factor. Of the redox electrolytes tested ($\mathrm{S^{2-}/S_x^{2-}}$, $\mathrm{I_3^-/I^-}$, $\mathrm{[Fe(CN)_6]^{3-/4-}}$ and $\mathrm{Fe^{2+/3+}}$ EDTA), the $\mathrm{[Fe(CN)_6]^{3-/4-}}$ couple was by far the most efficient in terms of charge transfer across the ITO/electrolyte interface. Optical-to-electrical conversion efficiencies (η) of 1.57% and 5.7% (~AM 1 illumination) were attained for PEC cells based on n- and p-Si substrates, respectively. Detailed tests have revealed long-term stability in $\mathrm{[Fe(CN)_6]^{3-/4-}}$ electrolytes once the ITO film thickness (≥50 Å) and solution pH (~12–14) were optimized. n-Si/ITO electrodes were used for the photooxidation of $\mathrm{Cl^-}$ from concentrated LiCl and NaCl electrolytes to illustrate the chemical inertness and stability of these electrodes. Catalytic modification of the ITO surface with $\mathrm{RuO_2}$ was found to be necessary to sustain $\mathrm{Cl_2}$ production. Values of η up to 2.7% were recorded with this PEC system at 100 mW/cm^2. Finally, the applicability of Si/ITO heterojunction electrodes for the photoassisted splitting of water was demonstrated. Preliminary experiments have revealed a 40% reduction in the threshold voltage required for water photolysis. Catalytic modification of the ITO surface was again a prerequisite for efficient performance of these electrodes. Pt and $\mathrm{RuO_2}$ electrocatalysts were used for p- and n-Si substrates, respectively. Experiments with ITO thin-film electrodes on inert Ti substrates show that the observed behavior of Si/ITO electrodes may be rationalized on the basis of electrocatalytic activity of the ITO/electrolyte interface biased by the ITO/Si heterojunction. Kinetics at this interface are a key factor and in the extreme case (e.g., regenerative systems based on the $\mathrm{I^-/I_3^-}$ redox couple) may nullify any voltage gained by illumination at the Si/ITO heterojunction.

A key problem with photoelectrochemical (PEC) devices for conversion and storage of solar energy is electrode stability.[1] Recent work has focused, therefore, on the strategy of depositing an inert layer (e.g., metal, polymer) on the semiconductor surface to inhibit electrolyte attack.[2-4] We describe here the performance and characterization of an alternative photoelectrode structure that facilitates the use of narrow band-gap semiconductor substrates in aqueous media. The model substrate that we have chosen to illustrate our approach is Si—mainly because of the advanced degree of technology that exists on this material. Figure 1 is a schematic of the electrode structure that we have employed, which comprises n- or p-Si substrates on which are deposited successive layers of $\mathrm{SiO_2}$ and indium tin oxide (ITO) by suitable means. As will be discussed below, we have also investigated catalytic

---

[†] Permanent Address: Department of Plastics Research, Weizmann Institute of Science, Rehovot, Israel.

[‡] Present address: Department of Electrical Engineering, Boston University, Boston, MA 02215.

(1) K. Rajeshwar, P. Singh, and J. Dubow, *Electrochim. Acta*, **23**, 1117, (1978).

(2) (a) Y. Nakato, T. Ohnishi, and H. Tsubomura, *Chem. Lett.*, 883 (1975); (b) Y. Nakato, K. Abe, and H. Tsubomura, *Ber. Bunsenges, Phys. Chem.*, **80**, 1002 (1976); (c) Y. Nakato, S. Tonomura, and S. Tsubomura, *ibid.*, **80**, 1289 (1976).

(3) K. W. Frese, Jr., M. J. Madou, and S. R. Morrison, *J. Electrochem. Soc.*, **128**, 1939 (1981).

(4) (a) R. Noufi, A. J. Frank, and A. J. Nozik, *J. Am. Chem. Soc.*, **103**, 1849 (1981); (b) F. R. Fan, R. L. Wheeler, A. J. Bard, and R. N. Noufi, *J. Electrochem. Soc.*, **128**, 2042 (1981).

0002-7863/83/1505-0324$01.50/0

Table I. Summary of Available Data on the Performance Parameters[a] of Solid-State Solar Cells Containing the Si/ITO Heterojunction

type of substrate	Si conductivity type	method of deposition of ITO layer	V_{oc}, V	J_{sc}, mA/cm^2	FF	η, %	ref
single crystal	n-Si	spray pyrolysis	0.534	45.06	0.47	11.3	12
	n-n$^+$Si	spray pyrolysis	0.500	32.0	0.65	10.4	18
	n-Si	spray pyrolysis	0.605	32.1	0.67	13.0	9a
	n-Si	electron beam	0.485	30.3	0.67	9.0	14
	p-Si	ion beam	0.526	34.0	0.79	14.1	19
	p-Si	ion beam	0.510	32.0	0.70	12.0	11a
polycrystalline	n-Si[b]	spray pyrolysis	0.500	39.56	0.46	9.1	12
	n-Si[b]	spray pyrolysis	0.500	29.0	0.71	10.3	9a
	p-Si[b]	ion beam	0.542	24.9	0.71	9.6	9a
	p-Si[b]	ion beam	0.522	33.3	0.79	13.7	20
	p-Si[c]	ion beam	0.498	29.3	0.77	11.2	20
	p-Si[d]	ion beam	0.487	28.4	0.74	10.3	21
	p-Si[c]	ion beam	0.420	21.0	0.71	6.3	11b

[a] AM 1 illumination (100 mW/cm^2). [b] Wacker Chemitronic. [c] Monsanto. [d] Silicon on Ceramic (Honeywell).

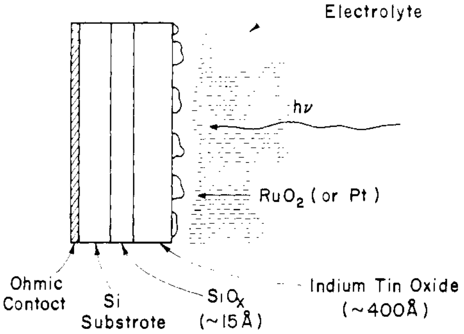

Figure 1. Schematic of the Si/ITO heterojunction photoelectrode structure employed in the present study.

modification of the ITO surface designed to offer specificity in Cl_2, O_2, and H_2 production in PEC storage systems.

While complications arising from direct contact of the semiconductor surface with the electrolyte (mainly photocorrosion) are largely avoided by the use of "hybrid" electrode structures such as those used in the present work (Figure 1) and in other studies,[2,5-7] two problems with this approach are recognized: (a) it is a Schottky barrier in an electrolyte and, as such, flexibility in varying barrier heights such as that available with conventional PEC systems is lost and (b) cell and electrode fabrication is considerably more complex than that for a simple PEC device. As we shall attempt to illustrate, however, these hybrid systems offer considerable versatility in that they offer possibilities for a variety of solar energy conversion schemes. Second, the present structure (Figure 1) has enabled the sustained use of Si under conditions (e.g., Cl_2 evolution) that would have otherwise resulted in its complete destruction. Third, respectable conversion efficiencies have been routinely obtained in nonoptimized regenerative systems with Si photoanodes. By way of contrast, our experience as well as that of others[8] has revealed wide variability in cell efficiencies in conventional PEC systems for a given semiconductor/electrolyte combination. This variability is undoubtedly the consequence of direct contact of the semiconductor surface with the electrolyte. This contact introduces complicating effects that are often difficult to control.

The Si/ITO Heterojunction. The Si/ITO interface has been the focus of much attention[9] in work related to the development of solid-state solar devices. Both n- and p-type Si substrates can be used with ITO, although the rectifying characteristics of the heterojunction seem to depend on the method employed to deposit the ITO layer. For this reason, photoelectrodes with p-Si in the present study were fabricated by neutralized Ar$^+$ beam sputtering while n-Si electrodes contained an ITO layer that was deposited by spray pyrolysis. These techniques were previously known[11-14]

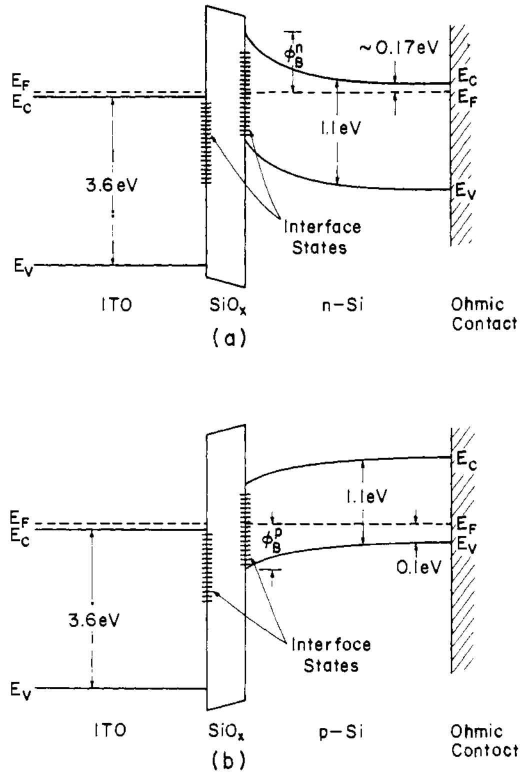

Figure 2. Equilibrium energy-band diagrams for (a) n-Si/ITO and (b) p-Si/ITO heterojunctions. E_c = conduction band edge, E_v = valence band edge, E_F = Fermi level, $\phi_B{}^n$ = barrier height for n-type substrate and $\phi_B{}^p$ = barrier height for p-type substrate.

---

(5) (a) L. A. Harris, M. E. Gerstner, and R. H. Wilson, *J. Electrochem. Soc.*, **124**, 1511 (1977); (b) R. H. Wilson, L. A. Harris, and M. E. Gerstner, *ibid.*, **124**, 1233 (1977).

(6) (a) S. Menezes, A. Heller, and B. Miller, *J. Electrochem. Soc.*, **127**, 1268 (1980); (b) B. Miller, A. Heller, S. Menezes, and H. J. Lewerenz in "Faraday Discussions 70: Photoelectrochemistry", A. J. Nozik, Ed. Oxford, England, 1980, p 223.

(7) J. S. Kilby, J. W. Lathrop, and W. A. Porter, U.S. Patent 4021323 (1977).

(8) E.g., H. S. White, H. D. Abruna, and A. J. Bard, *J. Electrochem. Soc.*, **129**, 265 (1982); see also references therein.

(9) For reviews for work in this area, see: (a) R. Singh, M. A. Green, and K. Rajkanan, *Sol. Cells*, **3**, 95 (1981); (b) J. Shewchun, D. Burk, and M. B. Spitzer, *IEEE Trans. Electron Devices*, **ED-27**, 705 (1980).

(10) S. Ashok, S. J. Fonash, R. Singh, and P. Wiley, *Electron Device Lett.* to be published.

(11) (a) J. DuBow, D. E. Burk, and J. R. Sites, *Appl. Phys. Lett.*, **29**, 494 (1976); (b) G. Cheek, N. Inoue, S. Goodnick, A. Genis, C. Wilmsen, and J. DuBow, *ibid.*, **33**, 643 (1978); (c) G. Cheek, A. Genis, L. Gobis, P. Smith, and J. DuBow, *Solid State Technol.*, February, 102 (1980); (d) A. Genis, P. Smith, K. Emery, R. Singh, and J. DuBow, *Appl. Phys. Lett.*, **37**, 77 (1980).

(12) J. Schunck and A. Coche, *Appl. Phys. Lett.*, **35**, 863 (1979).

to yield rectifying diodes with the two respective types of substrates (on the other hand, ion beam sputtered ITO often yields an ohmic contact on n-Si[10]). In all the cases, an interfacial SiO_x layer was intentionally incorporated in the heterojunction electrodes for two reasons: First, the layer provides a smooth transition from the semiconductor substrate to the overlying ITO and minimizes problems due to high interface state densities caused by mismatch in lattice constants, expansion coefficients, and other geometric factors. Second, this layer reduces the leakage (diode) current generated by the flow of majority carriers in the opposite direction and thereby improves the open-circuit voltage relative to an abrupt Si/ITO junction.[16] (The present electrodes, however, are described herein as "Si/ITO", with the recognition that the interfacial oxide layer is always present.)

Figure 2 illustrates energy band diagrams[13,17] that provide a reasonably good description of the electrical characteristics of n-Si/ITO and p-Si/ITO heterojunctions. As will become apparent from the ensuing discussion, the behavior predicted by these diagrams for PEC systems will have to be modified by the rate control exercised by the ITO/electrolyte interface. In this regard, the electrocatalytic efficiency of the ITO layer will be shown to be critically dependent on the specific redox electrolyte employed for regenerative PEC systems.

Table I provides a summary of available data on the performance of solid-state solar devices containing the Si/ITO heterojunction. These performance parameters are to be compared with values shown below for PEC systems based on this heterojunction. Further discussion on comparative aspects is postponed to a subsequent section.

The ITO Layer. While metal or polymer films have been employed in hybrid electrode schemes proposed by previous authors,[2-7] wide band-gap semiconductor oxides such as heavily doped SnO_2 or In_2O_3 offer the combination of high conductivity and high transparency. The indium oxide/tin oxide (90:10 mole ratio composition) system, in particular, is effective for solar cell applications for the following reasons: (a) It is electronically degenerate, thus reducing series resistance losses in the overlayer; (b) The index of refraction of ITO (~2.0) is such as to make it a partial antireflection coating on silicon; (c) ITO films are stable under most environmental conditions, are quite resistant to chemical attack, and adhere well to many substrates; (d) The wide band gap (3.6 eV) results in minimal visible light absorption in the oxide layer and thus allows most of the light to be absorbed in the junction area; and (e) ITO (as well as other oxide semiconductors) can be deposited at low temperatures so that interdiffusion (a problem with many metals; cf. ref 22) is minimized. The effective "zero-junction depth" minimizes any surface dead layer and improves short-wavelength response (the possibility of some surface damage induced by high-energy techniques such as ion beam sputtering, however, still exists; cf. ref 10).

The thickness of the ITO films in the present work ranged from 30 to 1000 Å, although most of the results below pertain to ~400-Å film thickness. This thickness was found to be optimum for PEC performance as discussed below.

Further details on ITO films may be found in reviews in the literature.[23,24]

Experimental Section

Single-crystal silicon (p-type, nominal resistivity: ~0.1 Ω cm) was obtained from commercial sources (Monsanto Corp.). The wafers (~15 mils thick) were passivated and metallized by Hewlett-Packard Inc., Loveland, CO. Approximately 1 μm of Al was deposited onto the back side for ohmic contact. The ion beam sputtering system used to deposit ITO has been described in previous publications from this laboratory.[11,19-21] The neutralized Ar^+ beam was first used to sputter-etch the Si wafer front surface with a beam energy of ~700 eV. Such a beam is known to penetrate the Si surface to ~10–20 Å. The hot-pressed ITO target (Materials Research Corp., MA) was then cleaned with the argon beam, after which a layer of SiO_x was grown on the Si substrate. ITO was then deposited on the Si wafer, which was maintained at a temperature of 373 ± 1 °C. A beam energy of 500 eV, O_2 partial pressure of 3×10^{-5} torr, and Ar partial pressure of 1×10^{-4} torr were nominally employed for electrode fabrication. Under these conditions, the interfacial layer of SiO_x is estimated to be ~15 Å thick. The thickness of the ITO film was measured on a Sloan Model 1000 quartz crystal monitor as well as by ellipsometry.

Ribbon silicon (Mobile Tyco, p-type, resistivity: ~0.1 Ω cm) was used in some experiments instead of single-crystal material and was fabricated into Si/ITO photodiodes in the same manner as described above.

An n-Si/ITO heterojunction electrode was kindly donated by Dr. J. Gobrecht. This electrode comprised single-crystal Monsanto substrate (resistivity: ~2 Ω cm) atop which layers of SiO_x (~15 Å thick) and ITO (400 Å thick) were successively deposited by spray pyrolysis. This technique has been detailed by previous authors in the literature.[13,18,25] Ohmic contacts were provided by vacuum-evaporated Au.

Individual PEC Electrodes (nominal geometric area: 0.1–0.5 cm^2) were scribed from the massive wafers in both cases described above. These electrodes were then mounted on Ti strips by using conducting Ag epoxy. The entire assembly was then insulated from the electrolyte (except for the portion to be exposed to light) with nonconducting epoxy resin as described elsewhere.[26] Prior to use in the PEC cell, the electrodes were thoroughly rinsed in deionized water (resistivity: 18 MΩ) and sometimes given a second rinse in dilute HCl for 10 s. Illumination of the electrodes was by ELH quartz–iodine projection lamps. The light intensities were either calibrated against a standard Si solid-state cell or monitored on an Ealing Corp. Model LIMS 920 radiometer/photometer. The intensities reported herein are not corrected for reflection losses from the ITO surface or for absorption in the cell wall and the electrolytes. Catalytic modification of the ITO surface with Pt was accomplished by controlled electrolysis of solutions of K_2PtCl_6 in distilled water (~0.1 M). The average thickness of the Pt deposits was estimated to be ~100 Å from the measured current densities and deposition times.[27] Scanning electron microscopy (SEM) revealed clusters of Pt on the ITO surface approximately 1–3 μm in diameter. For n-Si/ITO electrodes, RuO_2 electrocatalysts were employed for O_2 evolution and Cl^- oxidation (vide infra). These catalysts were incorporated on the ITO surface by treating the electrodes with a solution of $RuCl_3$ in acetone, followed by air-drying and subsequent oxidation in air at 400–500 °C for ~5 min. SEM pictures of the ITO surface thus treated again revealed that the catalyst deposition occurred in the form of macroscopic islands.

Standard three-electrode geometry was used in all cases for the PEC system reported here. Pt foil was used as the counterelectrode. All potentials are quoted with reference to the saturated calomel electrode (SCE). The instrumentation used for the electrochemical and PEC measurements was the same as that described previously.[26]

Redox electrolytes were prepared from Analar grade chemicals and deionized water. For studies on the $[Fe(CN)_6]^{3-/4-}$ couple, a 530-nm cutoff filter was used to minimize irreversible photochemical changes in the electrolyte on prolonged illumination. For the same reason, the cell was covered with Al foil except for a window through which electrode illumination occurred. For the same reason, the electrolyte was replenished at ~24-h intervals for extended stability "runs". Ferrous EDTA was prepared by dissolving ferrous perchlorate in 0.1 M disodium salt of ethylenediaminetetraacetic acid (EDTA). In this case as well as for

---

[13] S. Ashok, P. Sharma, and S. Fonash, *IEEE Trans. Electron Devices*, **ED-27**, 725 (1980).

[14] T. Feng, A. Ghosh, and C. Fishman, *J. Appl. Phys.*, **50**, 4972 (1979).

[15] P. A. Kohl, S. N. Frank, and A. J. Bard, *J. Electrochem. Soc.*, **124**, 225 (1977).

[16] For a discussion on the role of interfacial layers in solid-state cells, see, for example: (a) R. J. Stirn and Y. C. M. Yeh, *Appl. Phys. Lett.*, **27**, 95 (1975); (b) E. J. Charlson and J. C. Liu, *J. Appl. Phys.*, **46**, 9 (1975); (c) D. R. Lillington and W. G. Townsend, *Appl. Phys. Lett.*, **28**, 97 (1976).

[17] J. Shewchun, J. DuBow, A. Myszkowski, and R. Singh, *J. Appl. Phys.* **49**, 855 (1978).

[18] J. C. Manfacier and L. Szepeny, *Appl. Phys. Lett.*, **31**, 459 (1977).

[19] A. Genis, R. Singh, C. Osterwald, P. Smith, and J. DuBow, Proceedings of the 9th International Conference on Electron and Ion Beam Science and Technology Electrochemical Society, Princeton, NJ, 1980.

[20] A. Genis, P. Smith, C. Osterwald, R. Singh, and J. DuBow, *Electron Devices Lett.*, **1**, 143 (1980).

[21] A. Genis, R. Singh and J. DuBow, Proceedings of the Electron Devices Meeting, Washington D.C., IEEE, New York, 1980, p 206.

[22] S. Kar and W. E. Dahlke, *Solid-State Electron.*, **15**, 221 (1972).

[23] J. Vossen, *Phys. Thin Films* **9**, (1977).

[24] G. Hacke, *Annu. Rev. Mater. Sci.* **7**, 73 (1977).

[25] (a) T. Feng, A. Ghosh, and C. Fishman, *Appl. Phys. Lett.*, **35**, 266 (1979); (b) T. Nagatomo, M. Endo, and O. Onto, *Jpn. J. Appl. Phys.* **18**, 1103 (1979).

[26] P. Singh, K. Rajeshwar, J. DuBow, and R. Job, *J. Am. Chem. Soc.*, **102**, 4676 (1980).

[27] This thickness is very approximate because of the uncertainty induced in the measured currents due to H_2 evolution.

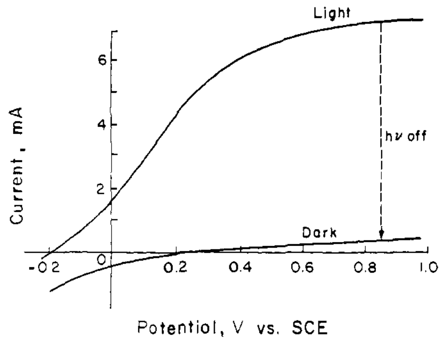

Figure 3. Steady-state current–voltage characteristics in the dark and under simulated AM 1 illumination for n-Si/ITO electrode (geometric area: 0.245 cm^2) in contact with 0.5/0.5 M $[Fe(CN)_6]^{3-/4-}$ couple (pH ~12). The ITO film thickness was ~400 Å, and the potential scan rate was 100 mV/S.

the $[Fe(CN)_6]^{3-/4-}$ couple, the pH of the electrolyte was adjusted either with NH_3, NaOH, or HCl.[21] Polysulfide electrolytes were prepared from mixtures of varying quantities of Na_2S, S, and NaOH in deionized water. Polyiodide electrolytes were prepared in similar fashion from Analar grade KI and I_2. In most cases, the cells were continually purged with inert gas during measurements to preclude deleterious oxidation reactions in the electrolyte. In experiments to monitor photooxidation of Cl^-, concentrated LiCl (15 M) solutions (pH ~6.6) were prepared according to procedures outlined by previous authors.[28] These electrolytes nominally contained ~0.05 M Cl_2, and the cells were sealed to prevent escape of Cl_2 gas. The rationale behind the use of these high ionic strength electrolytes is that the activity of H_2O and therefore the efficiency of photocorrosion can be significantly reduced.[28] NaCl solutions (5 M) were also used in experiments designed to test electrode stability.

Results and Discussion

Background Voltammograms in Inert Electrolytes. Background voltammograms were carried out on n-Si/ITO and p-Si/ITO electrodes in contact with inert buffered electrolytes with pH values ranging from ~2 to 14. The ITO layer thickness in these experiments was varied from 75 to 750 Å. The voltammograms in all cases were relatively featureless except at the extremes of potential excursions where they were bounded by H_2 evolution and water oxidation, respectively. It is doubtful whether the electrochemical characteristics of the ITO layer in these experiments were influenced to a significant degree by the underlying Si substrate in both the cases. A comparison with an electrode comprising an ITO layer deposited under practically identical conditions on an inert Ti substrate revealed no significant differences in behavior.

These results are in essential agreement with those reported by previous authors[29] for ITO electrodes in 1 N H_2SO_4 media. Additionally, however, our experiments with ITO electrodes in acidic media have revealed unstable behavior, especially with thin (<100 Å) layers. Under these conditions, prolonged electrolysis at negative potentials results in irreversible detrimental changes in the ITO layer that are clearly discernible to the naked eye. For this reason, most experiments with Si/ITO electrodes to be described below were performed in basic electrolytes (vide infra).

Photoeffects in Regenerative PEC Systems. Of the four redox electrolytes included for the present study, namely, polysulfide, I^-/I_3^-, $Fe^{2+/3+}$ (EDTA), and $[Fe(CN)_6]^{3-/4-}$, $[Fe(CN)_6]^{3-/4-}$ was by far the most effective. Figures 3 and 4 illustrate representative steady-state current–voltage curves for n-type and p-type Si substrates. The ITO film thickness was 400 Å and the electrolyte contained 0.5/0.5 M $[Fe(CN)_6]^{3-/4-}$ (pH ~13 ± 1) in these experiments. Anodic photocurrents for the n-type electrode and cathodic photocurrents for the p-type electrodes were observed at potentials well negative and positive, respectively, of the equilibrium redox potential (E_0 = 0.26 V).[30] These underpotentials represent a net conversion of optical to electrical energy in these devices. On the other hand, minimal photoeffects were observed in the cathodic currents and the anodic branch for the electrodes containing n-type and p-type substrates, respectively. This behavior is consistent with the photoeffects being entirely due to the generation of minority carriers (holes for n-type and electrons for p-type substrates, respectively). The concentration of majority carriers is not significantly affected by illumination.[31] That the photoeffects originated in the Si substrate and not in the ITO layer itself, was confirmed by measurements on ITO/Ti electrodes containing ITO layers of comparable thickness. No photoeffects were observed in these cases.

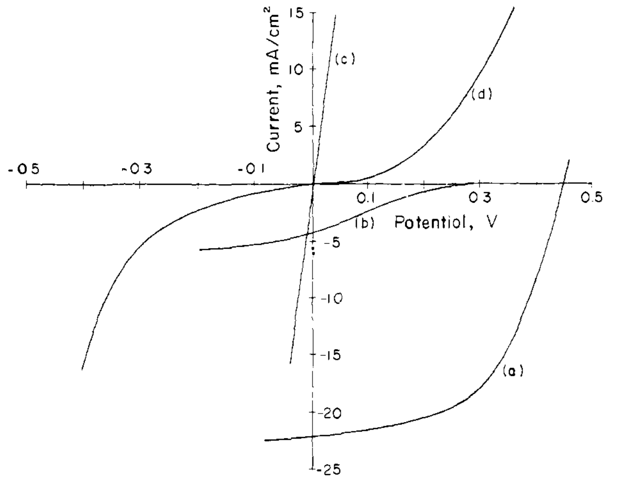

Figure 4. Steady-state current–voltage characteristics under 0.95 AMI illumination for a p-Si/ITO electrode (Mobile Tyco substrate, ITO film thickness: 400 Å in contact with 0.5/0.5 M $[Fe(CN)_6]^{3-/4-}$ couple (pH ~14) (curve a) and 1 M KI/0.05 M I_2 redox electrolyte (curve b). The dark currents in both cases were negligible on the current scale shown here. Also shown for comparison is the electrocatalytic activity of the ITO layer (thickness: 750 Å) deposited on an inert Ti substrate toward the $[Fe(CN)_6]^{3-/4-}$ (curve c) and I^-/I_3^- redox couples (curve d). The polarization curves for the ITO/Ti electrode in contact with the S^{2-}/S_x^{2-} and iron–EDTA redox systems were virtually superimposable on the curve for the I_3^-/I^- couple. Redox concentrations for curves c and d are the same as that used in the experiments with the p-Si/ITO electrode. Zero voltage refers to the equilibrium redox potentials of the two redox systems that were identical to within a few mV. The potential scan rate in these experiments was 20 mV/s.

The performance parameters for the examples shown in Figures 3 and 4 are as follows: short circuit current density (J_{sc}) = 18.67 mA/cm^2, open circuit voltage (V_{oc}) = 0.40 V, fill-factor (FF) = 0.21, corresponding to an AM 1 optical-to-electrical conversion efficiency (η) of 1.5% for the n-Si/ITO electrode. The corresponding values for the p-type electrode are J_{sc} = 22.0 mA/cm^2, V_{oc} = 0.45 V, FF = 0.55, and η = 5.7%. Comparison with the corresponding values for solid-state devices based on the same junction (cf. Table I) reveals the degradation in FF as the major factor in the reduced efficiency in the present PEC systems.

The key role that the redox electrolyte plays in the efficacy of charge transfer at the ITO/electrolyte interface is exemplified by the data shown in Figure 4 on the I^-/I_3^- redox couple. The PEC performance in this case is seen to be markedly inferior to the $[Fe(CN)_6]^{3-/4-}$ case discussed above, in spite of the fact that the E_0 values in the two cases are comparable. Photoenhancement of current flow is, however, seen in the cathodic polarization region. Interestingly enough, illumination of the p-Si/ITO heterojunction electrode results in light-induced suppression of anodic current flow. Essentially similar behavior was observed for the n-Si/ITO electrode with the polarities being revised, i.e., reduced overvoltage

---

(28) C. P. Kubiak, L. F. Schneemeyer, and M. S. Wrighton, *J. Am. Chem. Soc.*, **102**, 6898 (1980).

(29) N. Armstrong, A. Lin, M. Fujihara, and T. Kuwana, *Anal. Chem.* **48**, 741 (1976).

(30) The difference between the onset potentials for photocurrents on the n- and p-type substrates is ~0.8 V. This value is reasonably close to that expected from the band gap of Si (1.1 eV) minus the separation of the Fermi level from the conduction and valence band edges, respectively.

(31) H. Gerischer in "Physical Chemistry, An Advanced Treatise", Vol. IXA, H. Eyring, Ed., Academic Press, New York, 1970, p 492.

on illumination in the anodic region and minimal or "negative" photoeffects in the cathodic polarization regime.

Figure 4 also illustrates representative data from measurements on "control" ITO/Ti electrodes that provide further evidence for the extreme variance in charge-transfer kinetics in the $[Fe(CN)_6]^{3-/4-}$ and I_3^-/I^- redox systems. Overpotentials similar in magnitude to the I_3^-/I^- case (Figure 4) were also observed for the polysulfide and iron-EDTA redox couples. These in turn manifested as poor J_{sc}, V_{oc}, and FF values for the corresponding regenerative PEC cells on the basis of these couples.

The contrasting behavior observed for the $[Fe(CN)_6]^{3-/4-}$ redox couple vis-â-vis the I_3^-/I^-, polysulfide, and iron-EDTA redox systems, identifies a major loss mechanism in hybrid PEC structures as the overpotential at the surface layer/electrolyte surface. Charge transfer across this interface will have to be optimized (either by choice of a couple with fast kinetics or by suitable electrocatalytic modification of the surface layer as discussed below) so that the useful photovoltage gained at the Si/ITO interface is reflected in the ultimate performance of the overall PEC system. This important point is discussed further in a subsequent section.

It was hoped in these experiments that with a sufficiently thin ITO layer the photogenerated carriers arriving at the Si/ITO interface might traverse the ITO layer without losing all of their energy in nonelastic collisions within the ITO layer. For the p-Si/ITO system, for example, the average electron energy at the ITO/electrolyte interface would be greater than the Fermi level (redox potential) at that interface in equilibrium. Such an excess energy of the electrons could then be used to partially overcome the overpotential of the electrochemical reaction. If this occurred in practice, then the photoresponse for the p-Si/ITO electrodes in iodide electrolyte should improve as the ITO layer was made thinner since the initially poor photoresponse is due to the high overpotential at the ITO/iodide interface (cf. Figure 4). Such an improvement was not found even for ITO layers as thin as 30 Å, indicating that more or less complete thermalization of electrons occurred at or very close to the $p-Si(SiO_x)/ITO$ interface.

Electrode Stability. Tests of electrode stability were carried out for n-Si/ITO and p-Si/ITO electrodes in contact with the $[Fe(CN)_6]^{3-/4-}$ redox electrolyte. The variable parameter in these experiments was ITO film thickness and solution pH. For comparative purposes, the light intensity in these experiments was adjusted to yield an initial J_{sc} value of ~20 mA/cm^2 in all cases. For electrodes based on the n-Si substrate, no change in cell output occurred after >60 h of operation (>4 kC/cm^2 of charge passed). For p-Si when the ITO thickness was 50 Å or more, complete stability was found for times ranging from 70 to 110 hr, after which these experiments were discontinued. In the 30-Å case, J_{sc} dropped to 10 mA/cm^2 after ~3 h and continued to degrade thereafter. For this electrode, the degradation persisted in the dark. We believe that in this case electrolyte attack through the (possibly imperfect) ITO film is facilitated, resulting in pinhole formation as noted by previous authors.[15]

Further evidence for electrode stability was provided by the following observations: First, current-voltage curves similar to those shown in Figures 3 and 4 could be reproduced for the stable electrodes at the conclusion of the stability test. Second, pronounced hysteresis was absent in these data for the stable electrodes whereas the curves in the cathodic direction departed considerably from those on the reverse sweep for the photocorroded samples, e.g., p-Si/ITO (30 Å).

The electrolyte pH was >7 in all the above experiments. Acidic electrolytes resulted in visible etching of the ITO top layer and consequent irreproducibility in the current-voltage behavior (vide supra).

Photooxidation of Cl^- on n-Si/ITO Photoanodes. The capability of effecting highly energetic photooxidation reactions (i.e., those involving very positive redox potentials) at narrow band-gap semiconductor electrodes is presently hampered by the susceptibility of these materials to photocorrosion in aqueous media. As a test for the suitability of the present Si/ITO heterojunction electrodes for such applications, we chose the Cl_2Cl^- couple as a model redox system in conjunction with the n-Si/ITO photoanode. This couple has an important advantage over the others described in the preceding section in that it is optically transparent over most of the visible spectrum. Furthermore, the ability to sustain photooxidation of Cl^- offers possibilities of solar energy storage by coupling this reaction with proton reduction to induce the thermodynamically "uphill" dissociation of HCl into H_2 and Cl_2.

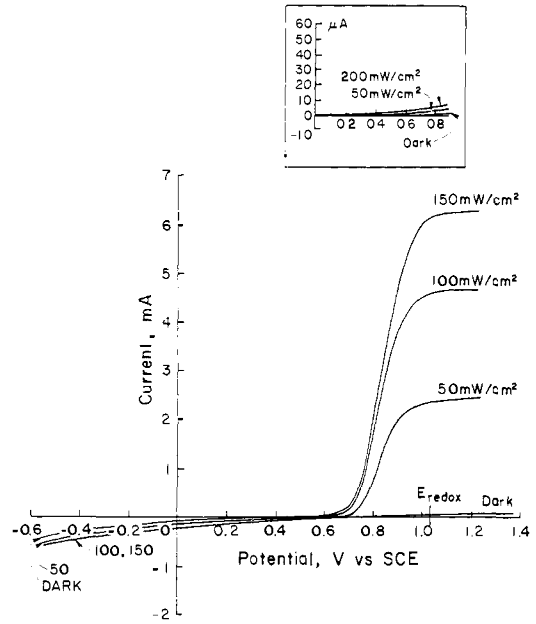

Figure 5. Potentiostatic current-voltage curves for a representative n-Si/ITO electrode modified with RuO_2 electrocatalyst in contact with magnetically stirred aqueous 15 M LiCl/0.05 M Cl_2 electrolyte. Inset: Behavior of the same electrode before electrocatalytic modification. Note the difference in the current scale in this case. To obtain current or power density, multiply by 5.26/cm^2.

Figure 5 illustrates typical I-V curves for n-Si/ITO photoanodes in contact with 15 M LiCl electrolyte. The data are compared for electrodes with and without electrocatalytic modification of the ITO surface with RuO_2. The dramatic improvement in the current efficiency in the presence of RuO_2 is reflected in the orders-of-magnitude increase in the current flow (from μA range to several mA, Figure 5) at comparable light intensities. More significantly, the photoanodic current onset (which is a function of light intensity) occurs at potentials well negative of the equilibrium redox potential, E_{redox}, which, in the present case, lies at +1.03 V. This shift is a direct measure of the up-conversion of visible light into useful electrical energy. The onset of photoanodic current flow is also accompanied by visible gas-bubble formation in the vicinity of the anode. This gas was identified as Cl_2 by chemical analyses.[32] The reaction at the counterelectrode is the reduction of Cl_2 to Cl^- ions or of protons to H_2 depending on the amount of Cl_2 present.[28] Performance parameters for the example shown in Figure 5 (100 mW/cm^2) were as follows: 17.1 mA/cm^2 at 0.87 V (equivalent photovoltage = 0.16 V based on E_{redox} = 1.03 V), yielding a conversion efficiency for photoassisted Cl_2 evolution of ~2.7%.

A test of photoelectrode stability seemed particularly relevant both because of the high oxidizing power of the products and to probe the mechanical effect of vigorous gas evolution that might conceivably damage the electrode surface. A stability test was therefore carried out in a 5 M NaCl aqueous solution. The electrode was maintained at +0.8 V under potentiostatic control corresponding to a current density of 14.3 mA/cm^2. A completely stable photoresponse (±5%) was observed for a period of 20 h,

---

(32) The oxidation of N,N-diethyl-p-phenylenediamine indicator by free chlorine was used for these analyses ("Drinking Water Analysis Handbook," Hach Chemical Co., Ames, Iowa, 1977, p 67). Spectrophotometric analyses revealed essentially 100% current efficiency for chlorine evolution.

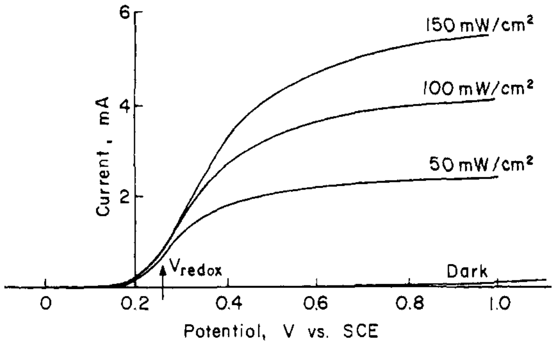

Figure 6. Steady-state current–voltage scans (scan rate: 100 mV/S) for catalytically modified (RuO_2) n-Si/ITO photoanodes in buffered NaOH electrolyte (pH ~12.5). Unmodified electrodes show negligible activity on the current scale shown in this figure.

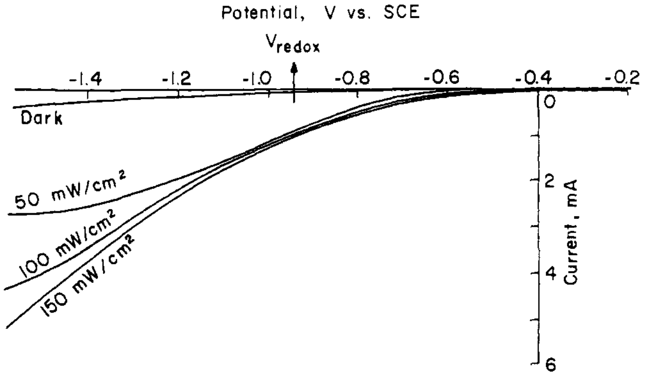

Figure 7. Short-circuit current density vs. time for n-Si/ITO (labeled 400 Å) and p-Si/ITO electrodes. The thickness refers to the ITO films. The behavior of a p-Si/ITO electrode with 400-Å ITO film thickness was virtually identical with the characteristics shown for the n-Si/ITO electrode.

after which the experiment was terminated.

Photoassisted Oxidation and Reduction of Water. The ultimate aim of a solar energy storage system would be to photosynthesize an energy-rich chemical (e.g., H_2 from H_2O) without the application of any external bias voltage. Systems constructed with n-$SiTiO_3$ as the photoanode have shown this useful property,[33] although the wide band gap of this material (3.4 eV) precludes efficient utilization of the solar spectrum. Efforts to utilize narrow band-gap semiconductors have been frustrated by their instability in aqueous media, although recent findings suggest that p-type semiconductors may be stable in this regard.[34] Of the progress to date on Si-based systems, mention may be made of the papers on the catalytic effect of electrodeposited metals[2] and on chemically modified electrode systems.[35]

We set out to examine the suitability of Si/ITO heterojunction electrodes for water splitting by constructing half-cells comprising n-Si/ITO and p-Si/ITO for the oxidation and reduction of water, respectively. Representative data are assembled in Figures 6 and 7 for n- and p-Si/ITO electrodes catalytically modified with RuO_2 and Pt, respectively, in contact with buffered electrolytes. The potentials required for water oxidation to O_2 is shifted by ~0.1 V negative of the equilibrium potential while that for water reduction to H_2[36] is shifted ~0.4 V positive of the H_2/H_2O potential. The reduction in the threshold voltage for water electrolysis implied by the data in Figures 6 and 7 would amount to ~40%. The photoactivity was minimal in the absence of electrocatalytic modification of the ITO surface in the two cases. Our current efforts are directed toward optimization of parameters associated with electrocatalytic modification and construction of a twin-photoelectrode PEC system based on the n-Si/ITO and p-Si/ITO heterojunctions.

General Discussion

While the variety of applications of Si/ITO photoelectrodes related to solar energy conversion and storage should become apparent from the data presented in the preceding sections, some general features of these systems deserve further discussion. The observed behavior of these heterojunction electrodes can be rationalized by using current models for semiconductor/insulator/semiconductor solar cells[9] in series with a metal/electrolyte junction. In this respect, ITO is equivalent to a transparent metal. Only in the presence of reasonably facile charge transfer at this interface (as is obviously the case with the $[Fe(CN)_6]^{3-/4-}$ couple and the catalytically modified electrodes) is the photovoltage developed at the Schottky barrier between the Si and the ITO layer (~0.4–0.6 V, cf. Table I) manifested usefully in the observed I–V characteristic for the various electrolyte systems examined in the present study. In all the other cases, this photovoltage is considerably reduced by overvoltage losses in current flow across the ITO/electrolyte interface.[37]

The current enhancement in the presence of light in the anodic region and cathodic region, respectively, for n- and p-type substrates and the minimal photoeffects in the opposite quadrants of the *I–V* curves (e.g., Figure 3) are readily understood in terms of minority-carrier generation in the Si layer. Creation of holes in n-Si should assist the flow of electrons from the reduced redox species into this layer via the intermediate ITO and SiO_x regions. Similarly, the photogenerated electrons on p-Si can enhance the cathodic current flow from the ITO layer into the electrolyte. In the dark, the electrochemistry is determined only by the characteristics of the ITO layer (cf. Figure 4). On illumination, the underlying Si substrate serves to "photobias" the ITO layer.

Our data on the photooxidation of Cl^- ions on catalytically modified n-Si/ITO electrodes demonstrate the extreme ruggedness of the latter. Although layer chalcogenides have shown a similar degree of stability under these conditions,[28] the present approach has permitted the use of Si substrates (for which an advanced degree of technology for fabrication of efficient polycrystalline material already exists, unlike the case of the former; cf. ref 38) and furthermore exploits the known affinity of certain oxide electrode surfaces toward Cl_2 evolution.

While the proof-of-concept data in Figures 6 and 7 conclusively show that photoassisted splitting of water can indeed be carried out on Si/ITO electrodes, it seems unlikely that the requirements of a combined photovoltage greater than 1.23 V will be met by the use of Si substrates. (Even on the optimistic assumption that there will be no intrinsic losses in a twin-photoelectrode system and taking the presently attainable maximum V_{oc} value of 0.6 V, the net photovoltage from such a system would still be only ~1.1–1.2 V.) One way out of this difficulty would be to use CdSe/ITO or InP/ITO junctions in place of either one or both of the Si/ITO electrode pair. Such systems have shown higher V_{oc} values than the Si/ITO heterojunction.[9a]

Summary and Conclusions

While the original impetus for this study was to find an alternative approach for stabilizing Si photoelectrodes in aqueous media, the results described herein also underline the wide variability in behavior encountered in the use of heterojunction (or Schottky barrier) electrodes in PEC systems. These systems can

---

(33) M. Wrighton, A. Ellis, P. Wolczanski, D. Morse, H. Abrahamson, and D. Ginley, *J. Am. Chem. Soc.* **98**, 2774 (1976).

(34) A. Heller, *Acc. Chem. Res.* **14**, 156 (1981), see also references therein.

(35) R. N. Dominey, N. S. Lewis, J. A. Bruce, D. C. Bookbinder, and M. S. Wrighton, *J. Am. Chem. Soc.* **104**, 467 (1982); see also references therein.

(36) H_2 evolution was confirmed by gas chromatographic (GC) measurements, cf. M. V. Rao, K. Rajeshwar, V. R. Pai Verneker, and J. DuBow, *J. Phys. Chem.* **84**, 1987 (1980). Attempts to monitor O_2 evolution using our GC system were not successful. A similar difficulty was experienced in the aforementioned study. Part of the problem could also be adsorption of O_2 on the ITO surface.

(37) The overvoltage will be developed across the Helmholtz layer at this interface in a direction (positive for n-type substrate and negative for p-Si) that will oppose the underpotential developed by light.

(38) D. S. Ginley, R. M. Biefeld, B. A. Parkinson, and K. Keung-Kam, *J. Electrochem. Soc.* **129**, 145 (1982).

be modeled as a series combination of a solid-state photovoltaic cell and a metal/electrolyte interface. A crucial factor in their performance is the efficacy of charge transfer at the overlayer/electrolyte interface. In the presence of fast kinetics at this interface, performance approaching that of the corresponding solid-state device can be realized. Kinetic hindrance to charge transfer at the overlayer/electrolyte interface manifests as overvoltage losses that reduce the photovoltage gained at the heterojunction. An important advantage with the use of heterojunction electrodes in PEC systems is the possibility of solar energy storage, which is obviously not offered by the corresponding solid-state device. Further improvements in catalytic modification of the ITO surface are, however, needed before the performance of PEC systems based on the Si/ITO heterojunction can match that of solid-state devices based on this interface.

Acknowledgment. This research was partially supported by a grant (XS-0-9272-1) from the Solar Energy Research Institute.

Registry No. Si, 7440-21-3; silicon oxide, 11126-22-0; indium tin oxide, 50926-11-9; Pt, 7440-06-4; RuO_2, 12036-10-1.

Recoil Tritium Reactions with 1,2-Difluoroethylenes

E. E. Siefert, D. D. Smith, R. E. Tricca, P. M. Ayoub, and Y.-N. Tang*

Contribution from the Department of Chemistry, Texas A&M University, College Station, Texas 77843. *Received June 29, 1982*

Abstract: Recoil tritium reactions with *cis*- and *trans*-CHF=CHF have been studied. The results indicate that the majority of the tritium-labeled parent molecules are formed via the direct T-for-H substitution process and that the geometric isomers are formed via unimolecular isomerization of the excited parent molecules. On the other hand, the recoil tritium addition process will give rise to an excited radical that immediately converts to a bridged complex. Such a bridged complex may either isomerize to effect a net 1,2 F-atom migration to give $CHT{=}CF_2$ as the final product or expel an F-atom to form CHT=CHF.

Recoil tritium atoms interact with π bonds in olefins very readily, giving rise to tritium-labeled radicals.[1-10] With enough excitation, such radicals may decompose by eliminating certain chemical entities to restore the π bond and form either the original or a different olefinic species as the final product.[4,5] Otherwise, it may be scavenged or it may undergo typical chemical interactions of free radicals in the reaction system. In the literature there are a number of studies devoted to the reactions of recoil tritium atoms with alkenes, but similar studies with substituted olefins are extremely rare.[1-10] In 1961, Urch and Wolfgang investigated the *cis*- and *trans*-dichloroethylene systems and obtained C_2H_2TCl as the major product, which probably arose from the following addition–elimination mechanism.[11]

$$\mathrm{T + CHCl{=}CHCl \rightarrow (CHTCl{-}CHCl\cdot)^*} \qquad (1)$$

$$\mathrm{(CHTCl{-}CHCl\cdot)^* \rightarrow CHT{=}CHCl + Cl} \qquad (2)$$

For the very small amount of *cis*- and *trans*-CHCl=CTCl observed in their experiments, the ratio of the isomers is about a factor of 2 in favor of the retention of the original geometric configuration. Similar favoritism is also detected in the recoil tritium studies with *cis*- and *trans*-2-butene performed by Rowland and co-workers.[7,8] Very recently, King and Wai have extended the recoil tritium reactions with *cis*- and *trans*-1,2-dichloroethylene to the liquid phase and have shown that the ratio of the isomers is more than a factor of 10 in favor of the isomer with the original configuration.[12] This means that hot T-for-H substitution at the ethylenic C–H bond proceeds with almost complete retention of configuration.

In the present work, recoil tritium reactions with *cis*- and *trans*-CHF=CHF have been studied. The results indicate that the majority of the tritium-labeled parent molecules are formed via the direct T-for-H substitution process. It confirms that substitution at the ethylenic C–H bonds proceeds predominantly with retention of configuration.[12] Furthermore, the results show that the CHTFCHF· radical formed from the recoil tritium addition process will undergo a 1,2 F shift to give $CHT{=}CF_2$ as a final decomposition product.[13] Although the shift of Cl and Br atoms in free radicals has been well established for at least two decades,[14,15] this is definitely the first unambiguous evidence for the occurrence of the F-atom shift in fluorine-containing radicals.[16,17]

Experimental Section

General Procedure. These experiments were performed by using the standard techniques employed in studying recoil tritium reactions.[1,18] Gaseous samples of the desired pressure that contained ^3He, the parent compound, and the desired additives were prepared by standard high-vacuum techniques and sealed in bulbs of about 20 mL in volume. The samples were irradiated at the Texas A&M Nuclear Science Center reactor for 10 min with a neutron flux of about 1×10^{13} n cm^{-2} s^{-1}. A set of 10 samples were generally irradiated with a rotisserie to normalize the neutron flux of the samples. In some sets, two pure n-C_4H_{10} samples were included as standards to allow for the calculation of absolute yields of products. In all these experiments tritium was produced in situ via

---

(1) Y.-N. Tang in "Isotopes in Organic Chemistry", Vol. 4, E. Buncel and C. C. Lee, Eds., Elsevier, Amsterdam, 1978, p 85.

(2) D. S. Urch, *MTP Int. Rev. Sci., Inorg. Chem., Ser. One*, *8*, 149 (1972); Ser. Two, *8*, 49 (1975).

(3) F. S. Rowland, in "Molecular Beam and Reaction Kinetics", Ch. Schlier, Ed., Academic Press, New York, 1970.

(4) K. L. Mahan and J. K. Garland, *J. Phys. Chem.*, **73**, 1247 (1969).

(5) K. L. Mahan and J. K. Garland, *J. Phys. Chem.*, **75**, 1031 (1971).

(6) D. S. Urch and R. Wolfgang, *J. Am. Chem. Soc.*, **81**, 2025 (1959).

(7) E. K. C. Lee and F. S. Rowland, *J. Inorg. Nucl. Chem.*, **25**, 133 (1963).

(8) R. Kushner and F. S. Rowland, *J. Phys. Chem.*, **75**, 3771 (1971).

(9) A. J. Johnston and D. S. Urch, *J. Chem. Soc., Faraday Trans. 1*, **69**, 1173 (1973).

(10) A. J. Johnston and D. S. Urch, *J. Chem. Soc., S. Faraday Trans. 1*, **69**, 1186 (1973).

(11) D. S. Urch and R. Wolfgang, *J. Am. Chem. Soc.*, **83**, 2997 (1961).

(12) W. G. King and C. M. Wai, *Radiochem. Radioanal. Lett.*, **30**, 27 (1977).

(13) E. E. Siefert and Y.-N. Tang, *J. Chem. Soc., Chem. Commun.*, 814 (1980).

(14) C. Walling in "Molecular Rearrangements", Vol. 1, P. de Mayo, Ed., Wiley, New York, 1963, p 407.

(15) R. K. Freidlina in "Advances in Free-Radical Chemistry", Vol. 1, G. H. Williams, Ed., Logos Press, 1965, p 211.

(16) W. Guillory and G. H. Andrews, *J. Chem. Phys.*, **62**, 3208 (1975).

(17) See, for example, W. J. Feast, R. R. Hughes, and W. K. R. Musgrave, *J. Fluorine Chem.*, **10**, 585 (1977).

(18) J. K. Lee, E. K. C. Lee, B. Musgrave, J. W. Root, Y.-N. Tang, and F. S. Rowland, *Anal. Chem.*, **34**, 741 (1962).

0002-7863/83/1505-0330$01.50/0